International Journal of High Speed Electronics and Systems
Vol. 17, No. 3 (2007) 585–591

World Scientific
www.worldscientific.com

INFRARED QUANTUM-DOT DETECTORS WITH DIFFUSION-LIMITED CAPTURE

N. VAGIDOV, A. SERGEEV, and V. MITIN

ECE Department, University at Buffalo, The State University of New York, 312D Bonner Hall, Buffalo, NY 14260, USA
nizami@eng.buffalo.edu
asergeev@eng.buffalo.edu
vmitin@.buffalo.edu

Employing Monte-Carlo simulations we investigate parameters and optimize geometry of IR quantum-dot detectors with diffusion-limited capture into the dots surrounded by potential barriers. Our results show that structures with modulation doping of interdot matrix provide an effective separation of the localized and conducting electron states. In these structures, the capture time is mainly determined by the quantum dot concentration and the height of potential barriers around dots. The capture is not sensitive to the dot positions. It also weakly depends on the electric field up to the characteristic value, at which significant electron heating allows hot electrons to overcome the barriers. Optimizing the carrier capture and transit times, we show that quantum-dot structures have a lot of potentials for increasing the photoconductive gain and for the development of IR room-temperature detectors.

Keywords: Quantum-dot photodetector; diffusion-limited capture; modulation doping; gain.

1. Introduction

Starting from the pioneering work,[1] various quantum-dot structures have been intensively studied as promising candidates for development of effective infrared photodetectors with numerous applications in middle and long-wavelength IR ranges.[2-5] It is expected that the quantum-dot structures can provide long lifetime of excited electrons, which in turn increases the photoconductive gain and leads to higher responsivity and higher operation temperature.[4-6] Capture processes in quantum-dot structures can be significantly suppressed by a proper choice of geometry of the structure and specific doping. The carrier lifetimes would strongly increase, if the dots would be separated from the "conducting channels" by the potential barriers created by means of the modulation doping. In our previous works[6-8] we considered various realizations of potential barriers and their effects on the detector performance.

In the current paper, we investigate a model of the photodetector operating at the room temperature, where the electron mean free path is relatively short and the photoelectron capture is determined by the electron diffusion in the field of potential barriers surrounding the charged dots.[8] In Ref. 8, we obtained a set of analytical results

related to the trapping cross-section at small electric fields applied to the structure. Here, we employ Monte-Carlo simulations to optimize the geometry of the IR quantum-dot detectors with diffusion-limited capture into the dots surrounded by potential barriers. We study the capture and transit times as functions of the dot positions, sensor geometry, and electric field applied. Finally, we calculate the photoconductive gain and discuss the optimal structures.

2. Theoretical Model

In theoretical model quantum dots are considered as ideal spheres of radius a that are located at distances $2b$ from each other in x-, y-, and z-directions. The interdot matrix is doped by donors, and electrons from ionized donors move into the quantum dots. The negative charge of electrons in the dots and positive charge of ionized donors outside of the dots ($r > a$) form the barrier potential, $V(r)$, shown in Fig. 1. The number, N, of trapped by quantum dots electrons is determined by the concentration of donors. For the case of $N >> 1$, we can exploit the model of the spherically-symmetric distribution of the charge and quasi-classical approximation for the electron Fermi energy. The electrostatic potential can be described in this approximation as

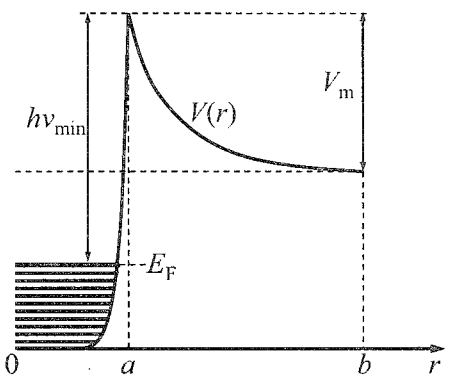

Fig. 1. Energy band diagram.

$$V(r) = V_0\left(\frac{b}{r} + \frac{r^2}{2b^2} - \frac{3}{2}\right), \qquad V_0 = \frac{eN}{\varepsilon b[1-(a/b)^3]}, \tag{1}$$

where ε is the dielectric permittivity of the interdot matrix. From Eq. (1) it is obvious that $V(r)$ is defined by several parameters, such as quantum dot radius, a, interdot distance, $2b$, number of electrons in quantum dot, N, that can be varied in wide ranges.

We consider room temperatures when the relaxation in quantum dots is fast enough to use the theoretical model with diffusion limited capture. The cross-section of electron capture is described by the following formulas:

$$\sigma = \pi\alpha\, a^2 \tilde{v}\, \exp\left(-\frac{eV_m}{kT}\right)\left(1 + \frac{3}{4}\frac{\alpha a}{\ell}F(V)\right)^{-1}, \tag{2}$$

$$F = a\, \exp\left(-\frac{eV_m}{kT}\right)\int_a^b \frac{dr}{r^2}\exp\left(\frac{eV(r)}{kT}\right), \tag{3}$$

where $\tilde{\nu}$ is the electron thermal velocity, ℓ is the electron mean free path, α is the probability for an electron at $r \le a$ to be captured by the quantum dot, and $V_m = V(a)$. Equations (2) and (3) were obtained for zero voltage applied to the structure. They are valid only if the positions of the turning points for the electron moving in the potential $V(r)$ are close enough to the quantum dot area. Satisfactorily this is reached at $a \ge 3$ nm. The formula for the electron capture time, τ_{capt}, is

$$\tau_{capt} = (N_d \sigma \tilde{\nu})^{-1}, \tag{4}$$

where N_d is the dot concentration. We use the same model for Monte-Carlo computations to investigate the dependence of electron capture times and gain of the photodetector on the concentration of dots and on the type of three-dimensional interdot space configurations.

3. Results of Monte-Carlo Simulations

We exploit Monte-Carlo program to simulate transport of three-dimensional electrons in InAs/GaAs photodetectors with the same concentration of InAs dots but with their different space locations in GaAs interdot matrix: (a) the cube configuration when all three distances between quantum dots $2c$, $2d$, and $2e$ in x-, y-, and z-directions, respectively, are equal to $2b$; (b) the parallelepiped configuration, which is flattened out in the direction of the voltage applied; and (c) the parallelepiped configuration, which is elongated in the direction of the voltage applied, (see Fig. 2). The concentration of quantum dots, $N_d = 1/cde = 1/b^3$, stays the same for all of three configurations. As we consider InGaAs dots embedded into the GaAs matrix, all parameters were taken for these materials. The Monte-Carlo simulation program is based on the model with electrons that may populate Γ-, L-, and X-valleys. It includes three major types of electron scatterings on: 1) acoustic, 2) polar optical, and 3) intervalley phonons. The electric field, applied in the y-direction provides strongly non-equilibrium electron distributions, but, at the same time, the increase of electron energy is not enough to initiate the avalanche processes or to modify significantly the potential barriers.

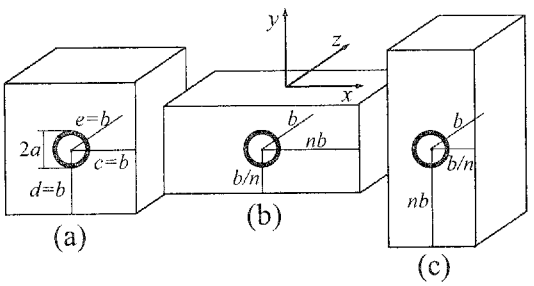

Fig. 2. Possible quantum-dot photodetector configurations: (a) the cube configuration: $c = d = e = b$; (b) the flattened parallelepiped configuration: $c = nb$, $d = b/n$, and $e = b$; and (c) the elongated parallelepiped configuration: $c = b/n$, $d = nb$, and $e = b$. Number n defines deviation from square configuration.

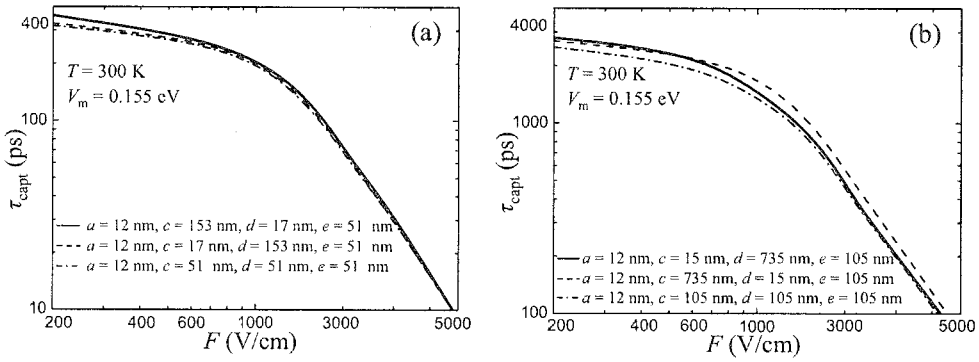

Fig. 3. Dependences of the photoelectron capture time on the electric field applied to the structures with the same value of dot radius and three different space configurations: (a) high and (b) low dot concentrations.

The results of simulations show that for the chosen variation of geometry the electron capture time, τ_{capt}, weakly depends on dot arrangement and that it is primarily determined by the dot concentration. In Figs. 3(a) and 3(b), we present dependences of the photoelectron capture times on the electric field applied to the structures with three space configurations (see Fig. 2) and dot concentrations of $1/(51\ \text{nm})^3 = 7.54\times10^{15}\ \text{cm}^{-3}$ (a) and $1/(105\ \text{nm})^3 = 8.63\times10^{14}\ \text{cm}^{-3}$ (b). As it is expected, the electron capture times for the cube configurations are slightly smaller (around 10 %) than that for parallelepiped configurations. The capture times for flattened and elongated parallelepiped configurations are almost the same. Thus, the capture time is not sensitive to dot arrangement. As it is seen in the Figs. 3(a) and 3(b), the capture time strongly depends on dot concentration and electric field, F. At electric fields greater than 1 kV/cm, the capture time, τ_{capt}, decreases by two orders of magnitude, while the electric field increases several times and such a behavior is practically insensitive to the structure geometry. Note, that the abrupt decrease of the carrier lifetime in the electric field explains the negative differential photoconductivity in quantum-dot detectors.[9]

Calculated dependences on the height of the potential barrier, V_m, for the considered three space configurations of quantum dots show similar behavior. At electric fields below 1 kV/cm, the dependence of the electron capture time on V_m is close to the exponential law that was obtained in the absence of the electric field (Eq. 2). In strong electric fields and low potential barriers, the capture time is practically independent on the barrier height [see Figs. 4 (a), 4(b), and 4(c)].

The main reason of such behavior is the heating of electrons in the applied electric field. At the characteristic field, average electron energy becomes comparable with the potential barrier. It is clarified in Fig. 5, where average energies, $\widetilde{\varepsilon}$, and population of Γ- and L-electrons are presented for electric fields up to 5 kV/cm. At room temperature the Γ-valley is mainly populated and at low electric fields, $F < 1$ kV/cm, electrons there stay weakly heated. At higher fields, above 3 kV/cm, the average energy of Γ-electrons, which mostly contribute to the electron transport (population of Γ-valley is almost 80 % even at

electric field F = 5 kV/cm; see Fig. 5), is almost linearly proportional to the electric field. As the average energy of Γ-electrons becomes comparable with the potential barrier, V_m, the electrons can be captured by quantum dots with much higher probability. As we can see from Figs. 3 and 4 electron capture times decrease with the increase of applied electric field, which causes the electron heating. The considered effects are fully described by Eqs. (2) and (3) if we will replace parameter kT by $\tilde{\varepsilon}$.

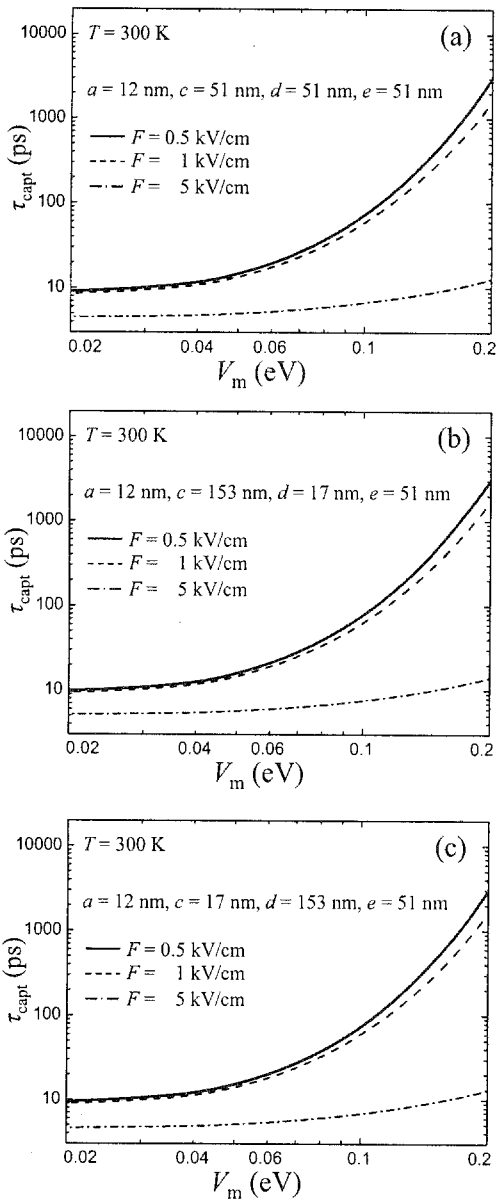

Fig. 4. Capture time dependences on the barrier V_m for three space configurations: cube (a), flattened (b) and elongated (c) parallelepipeds.

It is also important to note that at the room temperature, the electron mean free path ℓ is controlled by the inelastic electron scattering on the polar optical phonons. It is around 7 nm, which is smaller than the dot diameter. So, the electron capture is not sensitive to the relaxation processes inside of the dot. At the same time the mean free path is substantially smaller than the interdot distance. This is why the electron heating does not change the hierarchy of the relaxation lengths and the characteristic distances and, therefore, heating is practically independent on geometry of the structure.

The calculated electron capture time dependences on the electric field, F, for three space configurations allow us to analyze the gain dependences on electric field. The photoconductive gain is defined as a ratio of capture time, τ_{capt}, to the transit time across the active region of the device, τ_{tr}:

$$g = \tau_{capt} / \tau_{tr}. \qquad (5)$$

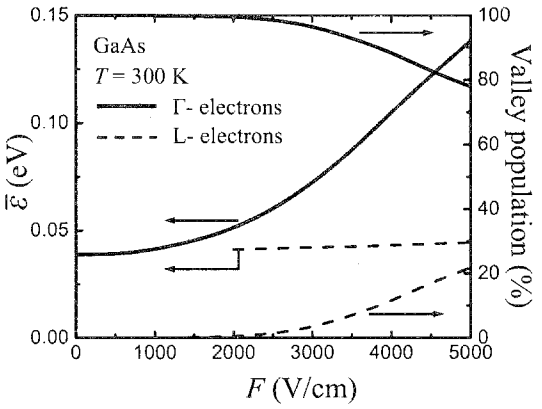

Fig. 5. The average electron energy and population of Γ- and L-valleys of GaAs by electrons as a function of the electric field, F.

Found in the process of Monte Carlo modeling average drift velocities and capture times for two quantum dot concentrations and three space configurations (Fig. 3) are used to calculate dependences of the photoconductive gain on the electric field, F at the fixed value of the potential barrier (see Fig. 6). Despite the differences in the dot concentrations and dot space configurations, the behavior of gain dependences in Figs. 6(a) and 6(b) are very similar. The gain reaches maximum value at electric field of ~1 kV/cm, which is also the characteristic field for the dependences shown in Fig. 3. At low electric fields, where capture time, τ_{capt}, is almost constant, the gain increases due to a decrease of the transit time, τ_{tr}; at high electric fields, the gain decreases due to exponential decrease of the capture time.

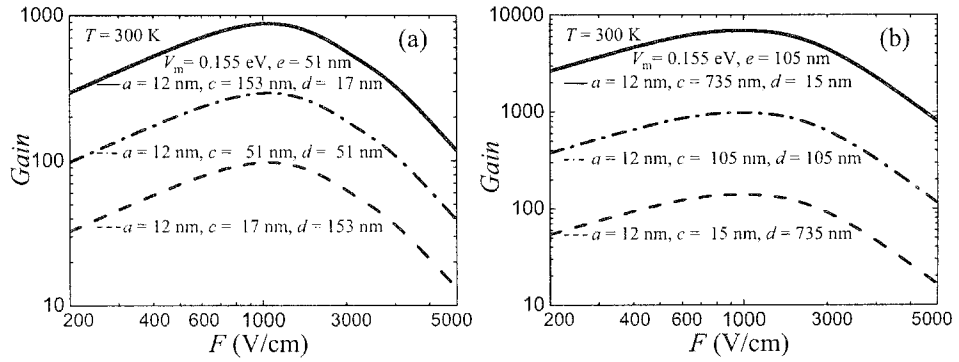

Fig. 6. Photoconductive gain per layer as a function of the electric field for two quantum dot concentrations and three space configurations that are shown in the Fig. 2.

In summary, the quantum dot structures with modulation doped barriers that separate localized and conducting electrons are promising candidates for the development of room-temperature IR photodetectors. Monte-Carlo simulations demonstrate weak dependence of capture times on the space geometry and electric field up to 1 kV/cm. The transit time substantially decreases in the configuration, which is flattened out in the direction of the voltage applied. Thus, the photoconductive gain is mainly limited by the electron heating. The probability of carrier capture substantially increases, when the

average electron temperature becomes comparable with the height of the potential barriers. The detector performance can be significantly improved by properly engineered potential barriers as well as by the optimal choice of quantum dot concentration, space arrangement, and operating regime. In particular, high barriers and structures flattened in the direction of the applied voltage [as in Fig. 2(a)] lead to a substantial increase of gain.

Acknowledgements

The research was supported by NYSTAR and PRF grants.

References

1. V. Ryzhii, *Semicond. Sci. Technol.* **11**, 759 (1996).
2. Lin Jiang, Sheng S. Li, Nien-Tze Yeh *et al.*, *Appl. Phys. Lett.* **82**, 1986 (2003).
3. W. Zhang, H. Lim, M. Taguchi *et al.*, *Appl. Phys. Lett.* **86**, 191103 (2005).
4. P. Bhattacharya, X. H. Su, S. Chakrabarti *et al.*, *Appl. Phys. Lett.* **86**, 191106 (2005).
5. J. Phillips, *J. Appl. Phys.* **91**, 4590 (2002).
6. V. V. Mitin, V. I. Pipa, A. V. Sergeev *et al.*, *Infrared Phys. and Technol.* **42**, 467 (2001).
7. V. Ryzhii, I. Khmyrova, V. Mitin *et al.*, *Appl. Phys. Lett.* **78**, 3523 (2001).
8. A. Sergeev, V. Mitin, and M. Stroscio, *Physica B* **316-317**, 369 (2002).
9. V. Ryzhii, *Appl. Phys. Lett.* **78**, 3346 (2001).